Transepithelial Water Permeability in Microperfused Distal Airways

Evidence for Channel-mediated Water Transport

Hans G. Folkesson, Michael A. Matthay, Antonio Frigeri, and A.S. Verkman

Departments of Medicine and Physiology, Cardiovascular Research Institute, University of California, San Francisco, California 94143-0521

Abstract

Water movement across the airway epithelium is important for regulation of the volume and composition of airspace fluid. A novel approach is reported here to measure osmotic and diffusional water permeability in intact airways. Small airways (100–200 μm diameter, 1–2 mm length) from guinea pig lung were microdissected and perfused in vitro using concentric glass holding and perfusion pipettes. For measurement of osmotic water permeability (P_f), the airway lumen was perfused with PBS (300 mOsM) containing a membrane impermeable fluorophore, fluorescein sulfonate (FS), and the airway was bathed in solutions of specified osmolalities. P_f determination was based on the change in FS fluorescence at the distal end of the airway resulting from transepithelial water transport. P_f was 4–5 $\times$ 10^{-3} cm/s at 23°C and independent of lumen flow rate (10–100 nl/min) and the magnitude and direction of the osmotic gradient (bath osmolality 50–600 mOsM). Temperature dependence measurements gave an activation energy of 4.4 kcal/mol (15–37°C). P_f was not altered by 0.3 mM $HgCl_2$ or 50 μM forskolin, but was increased to 31 $\times$ 10^{-3} cm/s by 100 μg/ml amphotericin B, indicating that osmosis is not limited by unstirred layers. Diffusional water permeability (P_d) was measured by H_2O/D_2O (deuterium oxide) exchange using the H_2O/D_2O-sensitive fluorescent probe aminonapthelane trisulfonic acid in the lumen. Measured P_d was 3–6 $\times$ 10^{-6} cm/s at 23°C, indicating significant restriction to water diffusion by unstirred layers. Antibody localization of water channels showed strong expression of the mercurial-insensitive water channel (AQP-4) at the basolateral membrane of airway epithelial cells. These results provide functional evidence that water movement across the distal airway epithelium is mediated by water channels. (*J. Clin. Invest.* 1996. 97:664–671.) Key words: aquaporin • water channel • osmosis • unstirred layers • fluorescence

Introduction

Substantial quantities of water move into the air spaces to replace water losses associated with respiration and move out of the air spaces in the neonatal lung and during resolution of pulmonary edema. Transepithelial transport of water is generally driven by osmotic gradients produced by active ion transport. In lung epithelia, major ion-transporting mechanisms include active Na^+ transport, which involves Na^+/K^+ pumps and Na^+ channels (1–4), and passive Cl^- transport mediated by CFTR Cl^- channels (5). The alveoli and distal airways comprise the majority of lung surface area available for transepithelial fluid movement. Transalveolar water permeability has been measured in an in situ perfused sheep lung model from the kinetics of osmotically induced water movement from blood to air space (6). Transalveolar osmotic water permeability was high and reversibly inhibited by $HgCl_2$, indicating a transcellular route for water movement through mercurial-sensitive water channels. No information is available about the water permeability of the distal airway.

Several molecular water channels (aquaporins) related to the major intrinsic protein of lens (7) have been cloned recently, some of which are expressed in lung (for review see references 8–10). Channel forming integral protein (CHIP)[1] is a 28-kD membrane-spanning glycoprotein expressed in erythrocytes, kidney proximal tubule, and thin descending limb of Henle, choroid plexus, ciliary body, and various water transporting epithelia and endothelia (11–14). In lung, CHIP28 is expressed on capillary endothelia (6, 12) and weakly on alveolar epithelia (6). CHIP28 functions as a mercurial-sensitive water-selective transporting protein; however, the identification of three phenotypically normal individuals who do not express CHIP28 makes uncertain its physiological significance (15). A second mammalian water channel (AQP2, reference 16) and an homologous protein (17) are expressed exclusively in kidney. A mercurial-insensitive water channel (MIWC or AQP-4) was cloned from rat lung (18) and human brain (19) and was immunolocalized to tracheal and bronchial epithelia, kidney collecting duct, ependymal cells, astrocytes in brain, colonic surface epithelia, and other epithelial and neuromuscular tissues (20, 21). A glycerol intrinsic protein (GLIP or AQP3, references 22–24) was cloned by three laboratories and functions as a glycerol- and possibly as a water-transporting protein. GLIP protein is coexpressed with MIWC in trachea, kidney, and intestine and is expressed without MIWC in epidermis, urinary bladder transitional epithelium, and conjunctiva (20, 21). Recently, another mercurial-sensitive water channel (AQP5) was cloned from salivary gland (25), in which the transcript was also expressed in lung, eye, and lacrimal gland. The

Address correspondence to Alan S. Verkman, Cardiovascular Research Institute, 1246 Health Sciences East Tower, Box 0521, University of California, San Francisco, CA 94143-0521. Phone: 415-476-8530; FAX: 415-665-3847; E-mail: verkman@itsa.ucsf.edu

Received for publication 9 August 1995 and accepted in revised form 8 November 1995.

J. Clin. Invest.

0021-9738/96/02/0664/08 $2.00
Volume 97, Number 3, February 1996, 664–671

1. *Abbreviations used in this paper:* ANTS, aminonapthelane trisulfonic acid; CHIP, channel forming integral protein; E_a, activation energy; FS, fluorescein sulfonate; GLIP, glycerol intrinsic protein; MIWC, mercurial-insensitive water channel; P_d, diffusional water permeability; P_f, osmotic water permeability.

contributions of these proteins to water movement across alveolar and airway epithelia is unknown (10).

The purpose of this study was to measure the fundamental water transport properties of intact distal airways: osmotic water permeability (P_f), diffusional water permeability (P_d), dependence of P_f on osmotic gradient size and direction, Arrhenius activation energy (E_a), and effects of mercurial inhibitors. Airways from rat, rabbit, mouse, and guinea pig were evaluated for these studies. The guinea pig was chosen because relatively long segments of viable distal airway (up to 2 mm) could be microdissected with minimal tissue trauma. An in vitro microperfusion technique, developed originally for microperfusion of kidney tubules, was modified for microperfusion of isolated distal airways. P_f was measured from the fluorescence of a membrane-impermeant luminal marker at the distal end of the airway in response to transepithelial osmotic gradients (26, 27); P_d was measured from the fluorescence of a D_2O (deuterium oxide)/H_2O–sensitive luminal marker in response to transepithelial D_2O gradients (28). In contrast to conventional radiotracer methods, the fluorescence approaches provide quantitative water permeability data in real time and without the need to collect fluid at the distal end of the airway. The results indicated a relatively high P_f and low E_a for distal airway water transport, providing functional evidence for transcellular movement of water through molecular water channels.

Methods

Isolation and perfusion of distal airway segments. Isolated segments of distal airways were microdissected from adult Dunkin-Hartley guinea pigs (n = 38 guinea pigs, 300–350 g; Simonsen, Gilroy, CA). The guinea pigs were anesthetized with pentobarbital (70 mg/kg), and the abdominal aortae were transected. After exsanguination, the lungs were removed through a midline sternotomy and filled to capacity with ice-cold PBS containing 1% albumin and 1 g/liter glucose (buffer A). The trachea was closed to prevent PBS leak. 60 ml of air was then injected with a 30 gauge hypodermic needle just beneath the visceral pleura to facilitate separation of airways from lung parenchyma. After a 20-min incubation on ice, larger airways were dissected free from parenchyma by gently pulling the parenchyma of the distal airways. The larger airways, which included the smaller airways of interest as branches, were further dissected to isolate individual distal airways. The microdissected distal airways were transferred by pipette to a storage container containing buffer A and maintained for up to 3 h on ice before experiments. The distal airways were never touched directly by the dissection or transfer instruments. This dissection method produced viable airway segments that excluded the vital stain Trypan blue. Airways without bifurcations over 1–2 mm length and of apparent diameter 100–200 μm were used for microperfusion.

A distal airway was mounted on a glass holding pipette by gentle suction. The lumen was then cannulated with a second, concentric pipette for luminal perfusion (Fig. 1). The perfusion pipette fit snugly in the airway lumen to prevent leakage of the luminal perfusate. Holding pipettes were pulled with a vertical pipette puller (Model 700c; David Kopf Instruments, Tujunga, CA) from R-6 glass tubing (O.D. 0.084″, I.D. 0.064″, length 8″; Drummond Scientific Co., Broomall, PA). The end of the pipette holding the airway was pulled to have an inner diameter of 100–200 μm with a gradual taper. Perfusion pipettes were pulled with a horizontal pipette puller (Model P87, Flaming/Brown Micropipette Puller; Sutter Instruments Co., Novato, CA) from R-6 glass tubing (O.D. 0.047″, I.D. 0.040″, length 8″; Drummond Scientific Co.). The tip to be introduced into the airway was pulled to approximate the airway inner diameter. The microperfused airway was held in a 100 μl laminar flow open chamber in which bath solution exchange time was < 0.5 s (27). The microperfusion apparatus and chamber were mounted on the x-y movable stage of an inverted epifluorescence microscope (Nikon Diaphot).

The luminal perfusion rate was maintained at 10–100 nl/min with a nanoliter infusion pump (Harvard Apparatus Inc., S. Natick, MA) driving a 50 μl Hamilton syringe which was connected to the perfusion pipette with polyethylene tubing. The bath solution was exchanged continuously at a rate of 5–10 ml/min. Bath fluid composition was changed by adjusting a five-way valve just proximal to the perfusion chamber. Lumen fluid composition could not be changed with this setup. For measurement of P_f, the luminal perfusate contained PBS and the membrane-impermeant fluorophore fluorescein sulfonate (FS, 5 mM; Molecular Probes Inc., Junction City, OR). Airways were bathed in PBS (isosmolar), PBS diluted with distilled H_2O (hypoosmolar), or PBS containing excess NaCl (hyperosmolar). Solution osmolalities were measured with a freezing-point osmometer (Model 3DII, Advanced Instruments Inc., Needham Heights, MA). For measurement of P_d, the luminal perfusate contained PBS (in H_2O) and the membrane-impermeant fluorophore aminonapthelane trisulfonic acid (ANTS, 5 mM; Molecular Probes Inc.). The fluorescence quantum yield of ANTS increases 3.2-fold when H_2O is replaced by D_2O (28). The bath solution contained either PBS (in H_2O) or isoosmolar "PBS" prepared in 100% D_2O. Bath temperature was controlled by a heating jacket around the infusion tubing and measured by an indwelling thermistor.

Quantitative epifluorescence microscopy. Fluorescence was excited and detected from a 150–200 μm diameter circular spot at the distal end of an unbifurcated airway, or near the distal end of an airway but proximal to any bifurcations (Fig. 1). Airways were viewed through a ×25 long working distance objective (numerical aperture 0.35; Leitz Wetzlar). Fluorescence was excited using a 100-W tungsten-halogen lamp powered by a stabilized DC power supply (Oriel Corp., Stratford, CT) in series with a 1.0 O.D. neutral density filter and an infrared blocking filter. For measurement of FS fluorescence, excitation was at 480±5 nm, with a 510-nm dichroic mirror and a > 530-nm emission cut-on filter (Fig. 1). For measurement of ANTS fluorescence, excitation was at 380±10 nm, with a 430-nm dichroic mirror and a > 530-nm cut-on filter. Fluorescence was detected by a photomultiplier (R928S; Hamamatsu Phototonics, Middlesex, NJ). The signal was amplified (Model 110; Ealing Corp., S. Natick, MA) and digitized by a 12-bit analog-to-digital converter (ADALAB; Interactive Microware, State College, PA) interfaced to a PC computer. The signal was hardware filtered by a single pole RC filter with a 0.3 s time constant. Data was acquired at 30 Hz and generally averaged over 1 s time intervals.

Determination of osmotic and diffusional water permeability. For calculation of apparent P_f and P_d, the airway was assumed to be a smooth right cylinder with surface area (A), obtained from the optically determined airway diameter (d) and length (L) (A = πdL). P_f was calculated from the relation (26),

$$P_f = -(V_o C_o / V_w A)\,[(C_o - C_L)/(C_o\, C_b C_L) + C_b^{-2} \ln[(C_L - C_b)\, C_o/(C_o - C_b)\, C_L]$$

where V_o is the initial lumen perfusion rate (cm³/min), V_w is the partial molar volume of water (18 cm³/mol), C_o is perfusate osmolality, C_b is bath osmolality, and C_L is calculated osmolality at the distal end of the airway. Because the fluorescence intensity of FS is linearly proportional to its concentration when [FS] < 5 mM (no self-quenching), C_L was determined from the product of C_o and the ratio of fluorescence intensities in the presence and absence of a transepithelial osmotic gradient.

P_d was calculated from the relation (28),

$$P_d = (V_o/A)\ \mathrm{In}\ C_{in}/C_{out}$$

where C_{in} is the fraction of H_2O in the luminal perfusate (C_{in} = 1.0) and C_{out} is the fraction of H_2O at the measuring area at the distal end of the airway. C_{out} was determined from an empirical relation gener-

ated from the reported dependence relative ANTS fluorescence on solution H_2O content (28): $C_{out} = 0.11\ f^2 - 0.91\ f + 1.79$, where f is the ratio of ANTS fluorescence measured with a PBS (H_2O) bath to that with a PBS (D_2O) bath.

Immunolocalization of MIWC. Polyclonal antibodies against a synthetic COOH-terminus peptide of MIWC (EKGKDSSGEVLSSV) were raised in rabbit and purified by peptide affinity chromatography (20). Guinea pig lungs were perfused with PBS and fixed in situ with PBS containing 4% paraformaldehyde. Lungs were removed, sliced, and postfixed for 4 h, cryoprotected overnight with PBS containing 30% sucrose, embedded in optimal cutting temperature compound, and frozen in liquid N_2. Cryostat sections (4–6 μm) were blocked for 10 min with PBS containing 1% BSA and then incubated with purified MIWC antibody (0.5 μg/ml) for 1 h at 23°C in PBS containing 1% BSA. Control experiments were performed using the purified antibodies preadsorbed with excess (> 10:1 molar ratio) synthetic peptide. Slides were rinsed with 2.7% NaCl and then with PBS. For immunoperoxidase detection, slides were incubated for 30 min with peroxidase-conjugated sheep anti–rabbit or mouse $F(ab')_2$ fragment (1:100, Amersham Corp., Arlington Heights, IL), rinsed, and then incubated with diaminobenzidine (0.5 mg/ml DAB in 0.01 Tris buffer, pH 7.6, containing 0.3% H_2O_2) for 20 min. Slides were counterstained with hematoxylin and photographed using Kodak Gold 100 film on an Optiphot microscope (Nikon Inc., Melville, NY).

Results

Water permeability was measured in microdissected distal airways which were perfused through the lumen with the membrane-impermeant fluorophores FS or ANTS. Fig. 1, *inset*, shows a microperfused airway *trans*-illuminated with dim light to visualize the airway and holding/perfusion pipettes, and *epi*-illuminated (485 nm) to excite FS fluorescence in a small spot near the distal end of the airway. Distal airways of 100–200 μm diameter were microdissected with lengths of up to 2 mm. There was no visible change in airway morphology under the various experimental conditions as described below.

P_f was measured from the change in FS fluorescence at the distal end of the airway in response to a transepithelial osmotic gradient. As solute-free water enters the airway lumen in response to an osmotic gradient (for lumen osmolality > bath osmolality), lumen FS concentration decreases along the axis of the airway lumen. Fig. 2 *A* shows relative FS fluorescence at the distal end of the airway during bath perfusion with PBS (290 mOsM), PBS diluted with H_2O (50 mOsM), and then again with PBS. Perfusion with hypoosmolar buffer resulted in a prompt fluorescence decrease in < 5 s, and reperfusion with PBS promptly returned fluorescence to the original level. As predicted from Eq. 1, the magnitude of the fluorescence decrease was smaller at higher lumen perfusion rates (Fig. 2 *B*) because of the decreased lumen transit time for each FS molecule. Calculated P_f values were independent of lumen perfusion rate in the range 10–100 nl/min (Fig. 2 *C*). Also, changes in bath flow rate in the range 3–10 ml/min did not affect P_f (data not shown). These results indicate absence of lumen or bath extracellular unstirred layers in the airway P_f measurements.

The dependence of airway P_f on the magnitude and direction of the osmotic gradient was examined. Fig. 3 *A* shows a representative fluorescence time course in which an airway was perfused at constant lumen flow with PBS containing 5 mM FS and bathed in solutions of indicated osmolalities. The fluorescence signal change was dependent on external osmolality: the magnitude of the signal decrease was greater for a bath osmolality of 50 mOsM than 200 mOsM, and the signal increased for the hyperosmolar (600 mOsM) bath (Fig. 3 *B*). Calculated P_f values (Fig. 3 *C*) indicated that airway P_f is relatively high, consistent with the presence of water channels, and independent of the magnitude and direction of the osmotic gradient.

Temperature dependence studies were carried out to investigate whether transepithelial airway water transport is chan-

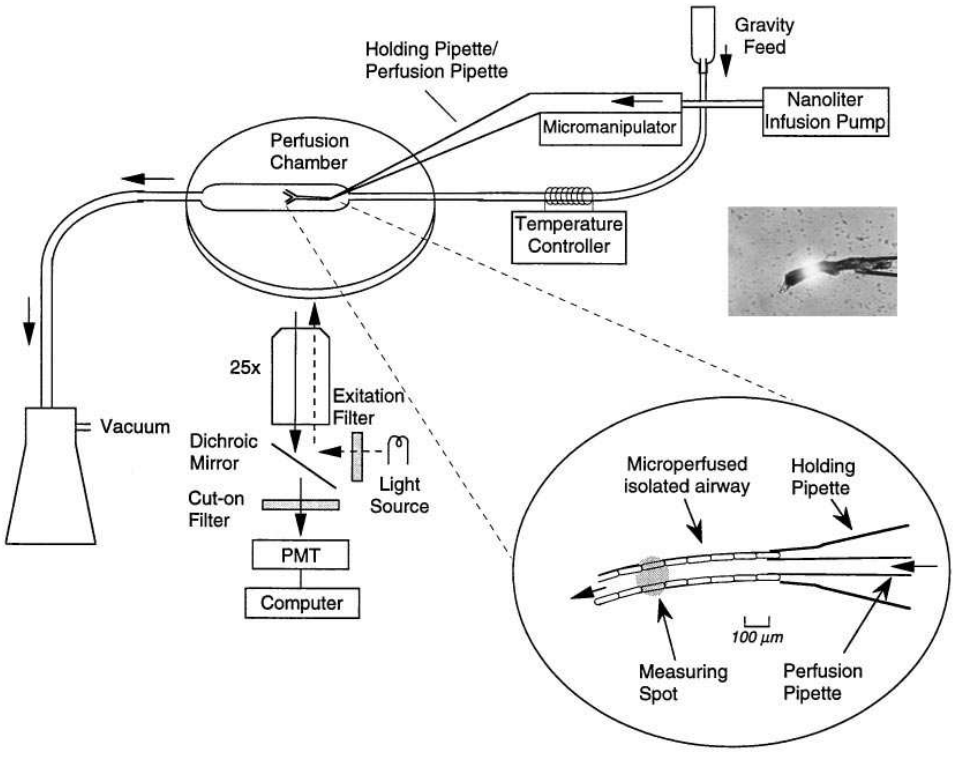

Figure 1. Schematic of the airway microperfusion instrumentation. The microdissected airway was perfused through its lumen at constant nanoliter/min rates and positioned in the bath of a perfusion chamber on the stage of an inverted epifluorescence microscope. Round inset shows an airway immobilized by the holding pipette and perfused with the concentric perfusion pipette. The measuring spot was positioned at the distal end of the airway, but before any bifurcations. See text for details. (*Square Inset*) Photomicrograph of a perfused distal airway. The airway was *trans*-illuminated with white light and *epi*-illuminated with monochromatic light for excitation of fluorescence at the distal end of the airway.

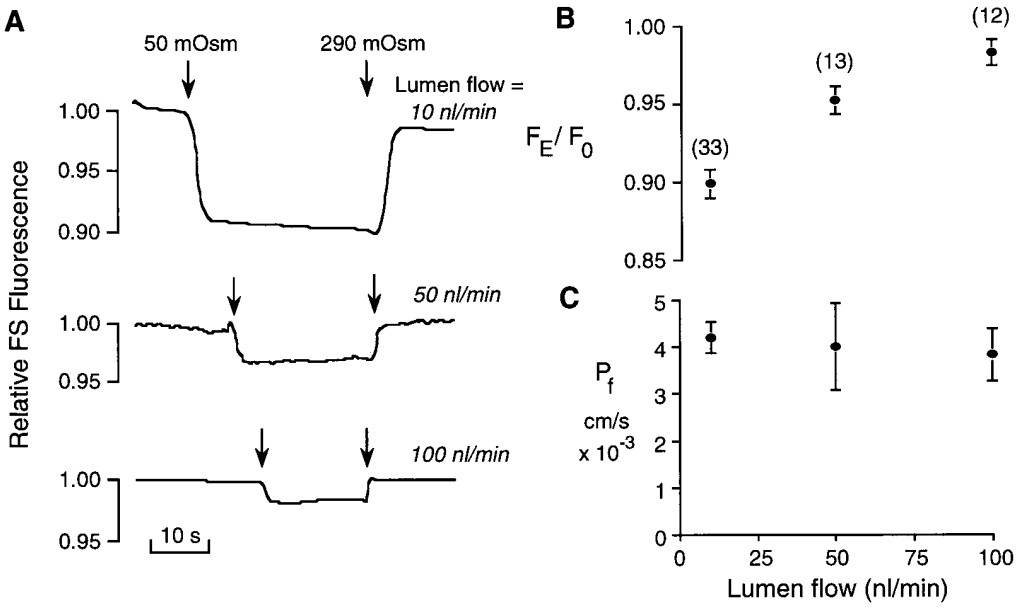

Figure 2. (*A*) Time course of luminal FS fluorescence at the distal end of the airway in response to changes in bath osmolality from 290 to 50 to 290 mOsM (*arrows*). Airways were perfused with 5 mM FS in PBS at 23°C. Lumen perfusion rate (lumen flow) is indicated. (*B*) Ratio of FS fluorescence (mean±SE, number of airways shows in parentheses, airways derived from 18 different animals) at the distal end of the airway with hypoosmolar bath solution (F_E) to that with PBS (F_o). (*C*) P_f was calculated from the data in *B* and airway geometry (differences not significant).

nel mediated. Fig. 4 *A* shows an Arrhenius plot of ln P_f vs. reciprocal absolute temperature. The slope of the plot gave a single E_a of 4.4±1 kcal/mol in the temperature range 15–37°C. This E_a is similar to that of 2–5 kcal/mol measured for osmotic water transport in erythrocytes and kidney tubule cell membranes which contain water channels, but much lower than that of > 10 kcal/mol in membranes not containing water channels (29, 30).

A low Arrhenius activation energy is consistent with water movement through molecular water channels and/or the presence of rate-limiting unstirred layers (29, 30). The independence of airway P_f on lumen and bath perfusion rates (see above) indicated the absence of extracellular unstirred layers; however, intracellular unstirred layers arising from flow-induced solute polarization in the cytoplasm were not ruled out. Our strategy to detect unstirred layers was to measure the increase in airway P_f upon addition of amphotericin B, a pore-forming agent which increases plasma membrane P_f without affecting unstirred layers (31); P_f would increase little if significant unstirred layers are present. Fig. 4 *B* shows that 100 μg/ml amphotericin B, a concentration that increased P_f in *Xenopus* oocytes threefold (31), increased airway P_f by approximately sevenfold. This finding indicates that unstirred layers comprise < 15% of the total transepithelial resistance to water flow. The conclusion that unstirred layers are absent in this preparation is also supported by the rapid change in luminal fluorescence in response to a change in bath osmolality.

Effects of possible inhibitors and activators of airway P_f were examined. To test for the involvement of mercurial-sensitive water channels at the basolateral surface of the airway epithelium, the effect of $HgCl_2$ was examined. Addition of 0.3 mM $HgCl_2$ to the bath solution, a concentration that inhibits water permeability in erythrocytes and kidney proximal tubule by >90%, did not cause inhibition of airway P_f (in cm/s × 10^{-3}:

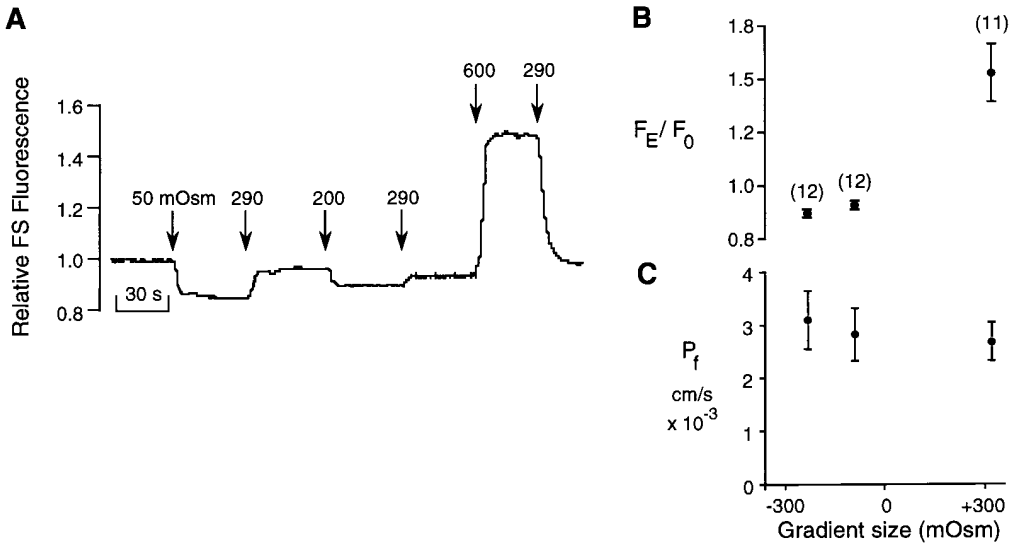

Figure 3. Dependence of airway osmotic water permeability on the magnitude and direction of the osmotic gradient. (*A*) Representative time course of FS fluorescence at the distal end of an airway in response to the indicated changes in bath solution osmolality. The airway was perfused with 5 mM FS in PBS at 10 nl/min, 23°C. (*B*) Measured F_E/F_o ratio (mean±SE, number of airways in parentheses, airways derived from nine different animals) as a function of osmotic gradient size. (*C*) Dependence of calculated P_f on osmotic gradient size (differences not significant).

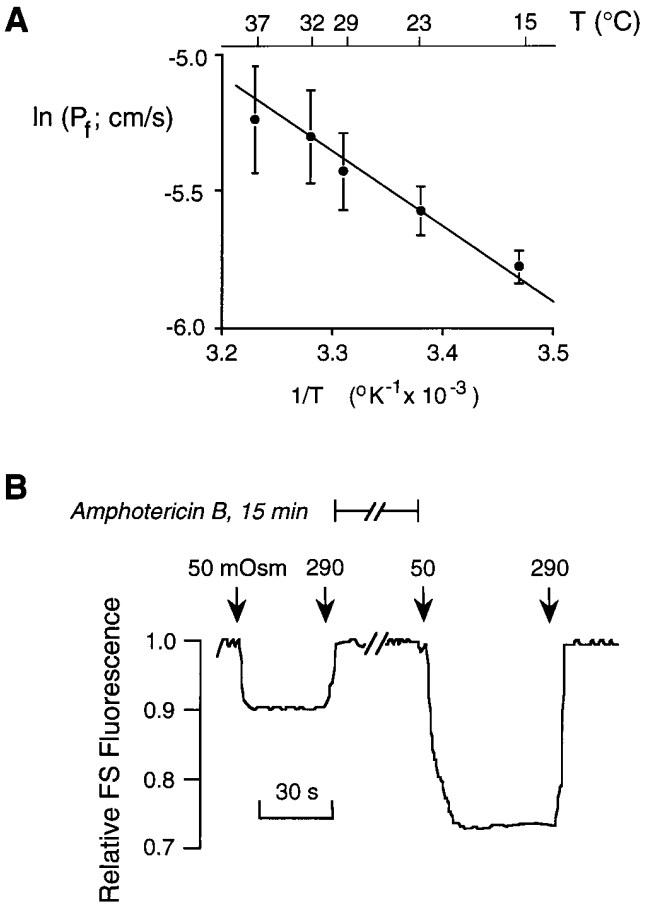

Figure 4. (*A*) Arrhenius plot of ln P_f (mean±SE, four to six measurements) vs. reciprocal absolute temperature (*1/T*). Fitted E_a was 4.4±1 kcal/mol (1 cal = 4.184J). (*B*) Effect of amphotericin B on airway P_f. The airway was perfused with 5 mM FS in PBS at 10 nl/min, 23°C. Where indicated, amphotericin B (100 μg/ml) was present in the bath solution for 15 min. Calculated airway P_f values before vs. after amphotericin B are given in the text.

4.2±0.3 [control] vs. 3.7±0.2 [+$HgCl_2$], n = 12). To test whether increased intracellular cAMP levels influenced airway P_f, the effect of forskolin was examined. At 50 μM forskolin, a concentration that stimulates airway epithelial cell cAMP to levels greater than those obtained with maximal isoproterenol, there was no effect on airway P_f (in cm/s × 10^{-3}: 3.8±0.2 [control] vs. 3.9±0.2 [+forskolin], n = 4).

The experimental method developed to measure airway P_f was applied to measure the transepithelial reflection coefficient for NaCl, σ_{NaCl}, an important quantity in transport physiology (32). The airway lumen was perfused at 10 nl/min with PBS containing FS, and bathed in PBS or an isosmolar solution containing PBS diluted sixfold with water and 240 mM sucrose. Sucrose is assumed to be an impermeant solute in distal airways with a reflection coefficient of unity. The lumen fluorescence signal changed by < 1% upon switching the bath between the PBS and PBS/sucrose solutions, giving a σ_{NaCl} of 1.00±0.02. A unity value for σ_{NaCl} indicates independent pathways for salt and water movement across the airway epithelium, and lack of solvent drag effects.

The ratio of osmotic-to-diffusional water permeability (P_f/P_d) is an independent parameter providing information on water channels; membrane P_f/P_d is unity for a solubility-diffusion water transport mechanism and > 1 in the presence of molecular water channels (29, 30). Airway P_d was measured using a membrane-impermeant fluorophore (ANTS), whose fluorescence quantum yield is 3.2-fold higher in a D_2O buffer than in an H_2O buffer (28). Airways were perfused in PBS (H_2O) containing 5 mM ANTS and bathed in PBS (H_2O) or isosmolar PBS (D_2O). As exchange of lumen H_2O for bath D_2O occurs, ANTS fluorescence increases along the axis of the airway. Fig. 5 shows a prompt increase in ANTS fluorescence at the distal end of the airway upon bath perfusion with PBS (D_2O); fluorescence returned to its original level upon reperfusion with PBS (H_2O). Calculated airway P_d values were (3.7±0.7) × 10^{-6} cm/s (10 nl/min lumen flow, n = 15), (3.0±0.7) × 10^{-6} cm/s (30 nl/min lumen flow, n = 3) and (3.6±1) × 10^{-6} cm/s (100 nl/min lumen flow, n = 3). These values are remarkably lower than airway P_f values and were not affected by amphotericin B (data not shown). Therefore, as is the case for kidney tubules and other epithelia (30), airway P_d is unstirred layer, rather than plasma membrane, limited. The unstirred layer resistance to water diffusion probably represents a combination of intracellular and extracellular aqueous and membrane barriers. Although measured airway P_d represents the actual diffusional water permeability of intact airways, it does not provide useful information about P_d in airway cell plasma membranes and is thus not suitable for calculation of intrinsic membrane P_f/P_d.

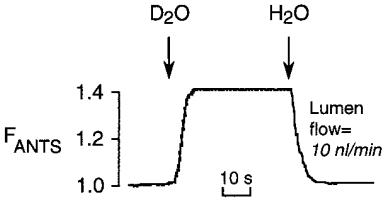

Figure 5. Measurement of airway diffusional water permeability by ANTS fluorescence. ANTS fluorescence was measured at the distal end of an airway perfused at 10 nl/min with PBS (H_2O) containing 5 mM ANTS at 23°C. Where indicated, bath PBS (H_2O) was replaced with isosmolar PBS in D_2O.

Immunolocalization studies were carried out to determine whether molecular water channels were expressed on distal airways. Immunostaining using antibodies against CHIP28, WCH-CD, and GLIP was negative. However, by immunoperoxidase, MIWC was strongly expressed at the basolateral membrane of distal airways in sections of guinea pig lung (Fig. 6 *A*). An immunodepleted control was negative (Fig. 6 *B*). MIWC was present in airway epithelia from trachea and bronchi, down to distal bronchioles, but was absent in terminal bronchioles, alveoli, and capillary endothelium.

Discussion

Functional studies were carried out to characterize the water permeability properties of intact distal airways. Transepithelial P_f was 6 × 10^{-3} cm/s at 37°C, and independent of lumen perfusion rate and the magnitude and direction of water flow. This P_f value is lower than that in the highly water permeable kidney proximal tubule (10–30 × 10^{-3} cm/s), the vasopressin-stimulated collecting duct (25 × 10^{-3} cm/s), and the alveolar epithelium (10 × 10^{-3} cm/s), but greater than that in the thin ascending limb of Henle (< 1 × 10^{-3} cm/s) and the unstimulated collecting duct (1 × 10^{-3} cm/s) (30). Water transport across the airway epithelium involves movement through se-

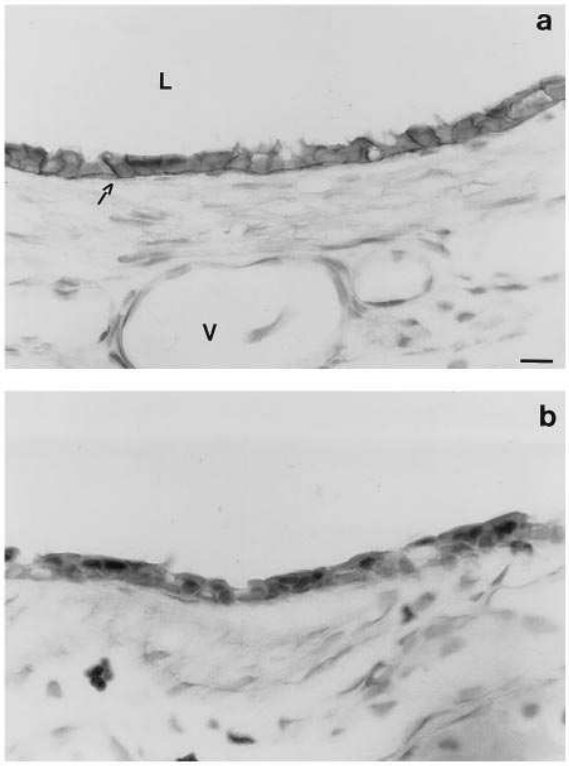

Figure 6. Immunoperoxidase localization of the mercurial-insensitive water channel in the basolateral membrane of guinea pig airways. (*A*) Lung section stained with MIWC antibody. (*B*) Immunodepleted control lung section. Scale bar: 10 μm. Labels denote: airway lumen (*L*), capillary vessel (*V*). Arrow indicates positive labeling at the basolateral membrane of airway epithelial cells.

rial resistances: the apical and basolateral membranes, and any extracellular or intracellular unstirred layers. Assuming (*a*) that the outer and inner airway surfaces consist of a relatively smooth surface, (*b*) equal apical and basolateral membrane P_f values, and (*c*) lack of significant unstirred layers, the P_f of individual airway cell plasma membranes is $\sim (6 \times 10^{-3}) \times 2 = 0.012$ cm/s at 37°C. A P_f value of > 0.01 has generally been taken to indicate the presence of water channels (8); however, there is considerable variability in biological and even artificial membranes. The low Arrhenius E_a for transepithelial airway P_f suggests a rate-limiting pathway for water movement involving water channels. It is noted however that the generalization of a low E_a for channel-mediated water movement and a high E_a for a solubility-diffusion transport mechanism is only empirical; E_a would be low if P_f is unstirred layer limited, when water movement occurs through or near other membrane proteins which do not function as specific water channels, or possibly in narrow water pores where significant water-pore interactions occur (8). The amphotericin B experiment indicated little or no unstirred layer effects for osmosis across distal airways. The relatively high P_f and low E_a in the absence of unstirred layers thus provides evidence for transcellular movement of water in the distal airway epithelium through water channels. High P_f/P_d has also been taken as evidence for water channels; however, as described in the results, airway P_d was found to be unstirred layer limited so that P_f/P_d cannot be interpreted in terms of intrinsic membrane properties.

The microperfusion and fluorescence assay techniques reported here should have applications in the measurement of constitutive and regulated transport of water and solutes across intact airways. Microperfusion of larger airways has been reported in three studies of ion transport based on transepithelial membrane potential measurement (33–35). It was shown that the airway actively absorbs Na^+ by a mechanism involving amiloride-sensitive Na^+ channels (33, 34) and that Cl^- is passively secreted (35). The airways in those studies were significantly wider (230–660 μm diameter) and shorter (0.4–1.5 mm length) than the distal airways examined in this study. The wider and shorter airways were suitable for measurements of membrane potential, but because of their low "length-to-surface" ratio, they are not suitable for measurement of transepithelial water or solute transport. The fluorescence assay technique used here involved slow luminal perfusion of the airway with a membrane-impermeant fluorophore whose fluorescence was dependent upon transepithelial volume flow (FS, for P_f measurement) or H_2O/D_2O exchange (ANTS, for P_d measurement). Airway perfusion with fluorescent indicators of ion concentration (e.g., Na^+, K^+, Cl^-, pH; reference 36) should enable quantitative real-time measurements of airway ion transport.

Various physiological roles have been proposed for fluid transport across the airway epithelium (37, 38). Based on the demonstration of active Na^+ transport (35), water transport across distal airways may be required to maintain a constant thickness of the fluid layer on the luminal surface of distal airways. This surface layer has been proposed to be an important determinant of airway stability under normal and pathological conditions (37, 38). High water permeability in the distal airways and alveolar epithelium probably also facilitates the reabsorption of pulmonary edema fluid (39). It is instructive to explore the quantitative implications of the airway P_f determined here. It has been estimated that the total alveolar surface area in human lung is 143 m^2 and that airway surface area is $\sim 1\%$ of alveolar surface area, ~ 1.4 m^2 (40). Given an evaporative water loss of 0.9 ml/min in the airways (41) and assuming that P_f of human and guinea pig airways are similar, it is calculated that an effective osmotic gradient of 14 mOsM exists across the intact airway epithelium. This estimate does not include possible effects of fluid movement up and down the airways. Nonetheless, although direct physiological measurements are needed to test this prediction, it is concluded from the relatively high airway P_f that very large osmotic gradients (600–900 mOsM, reference 41) cannot exist because the distal air spaces would rapidly fill with fluid.

The results here show relatively high transepithelial water permeability in distal airways but do not provide information about the water permeability of the individual apical and basolateral cell plasma membranes. The observation that bath amphotericin B strongly increases airway P_f might suggest that apical membrane P_f is greater than basolateral membrane P_f, as concluded in studies on cultured nasal epithelia (42); however, it is not known whether amphotericin B as used here is present in the apical membrane. Our studies thus do not rule out the possibility of a relatively low apical membrane P_f, as might be the case if the primary role of high basolateral membrane water permeability is to maintain constant intracellular osmolality and volume. Direct measurements of P_f on the apical and basal surfaces of intact airway epithelium are needed.

The strong expression of a molecular water channel,

MIWC, on the airway epithelium supports the hypothesis that high water permeability and water channels are important in lung physiology. MIWC has been shown to be a mercurial-insensitive, water-selective transporter expressed widely in fluid-transporting mammalian tissues (18, 20, 21, 43). Full-length MIWC protein is nonglycosylated and contains six membrane-spanning domains with its NH_2 and COOH termini in the cytoplasm (44). Recently, a human mercurial-insensitive water channel was cloned (19), which showed the unique feature of the expression of multiple protein isoforms produced by distinct but overlapping transcriptional units. Human MIWC has been localized to chromosome locus 18q22, which is distinct from the location of water channel homologs CHIP28, AQP-CD, and GLIP, which are not expressed in airways. Water channel AQP-5 is also expressed in lung (25) and is a possible candidate for an apical membrane water channel in airways, but has not yet been immunolocalized to specific cell membranes. Studies in transgenic knock-out animal models and in subjects with naturally occurring MIWC mutations will be required to establish with certainty the role of airway water channels.

Acknowledgments

We thank Dr. Lan-bo Shi for help in establishing the airway microperfusion methods.

This study was supported by National Institutes of Health grants HL51854, DK35124, HL42368, and DK43840 and grant R613 from the National Cystic Fibrosis Foundation. Dr. Folkesson was supported in part by a grant from the American Lung Association of California and Dr. Frigeri from the National Kidney Foundation of Northern California.

References

1. Olver, R.E. 1994. Fluid secretion and absorption in the fetus. *In* Fluid and Solute Transport in the Airspaces of the Lung. R.M. Effros and H.K. Chang, editors. Marcel Dekker, Inc. New York. p. 281–302.

2. Berthiaume, Y., N.C. Staub, and M.A. Matthay. 1987. Beta-adrenergic agonists increase lung liquid clearance in anesthetized sheep. *J. Clin. Invest.* 79: 335–343.

3. Effros, R.M., G.R. Mason, J. Hukkanen, and P. Silverman. 1988. New evidence for active sodium transport from fluid-filled rat lungs. *J. Appl. Physiol.* 66:906–919.

4. Matalon, S. 1991. Mechanisms and regulation of ion transport in adult mammalian alveolar type II pneumocytes. *Am. J. Physiol.* 261:C727–C738.

5. Boucher, R.C. 1994. Human airway ion transport. Part one. *Am. J. Respir. Crit. Care Med.* 150:271–281.

6. Folkesson, H.G., M.A. Matthay, H. Hasegawa, F. Kheradmand, and A.S. Verkman. 1994. Transcellular water transport in lung alveolar epithelium through mercury-sensitive water channels. *Proc. Natl. Acad. Sci. USA.* 91:4970–4974.

7. Reizer, J., A. Reizer, and M.H. Saier. 1993. The MIP family of integral membrane channel proteins: sequence comparisons, evolutional relationships, reconstructed pathway of evolution, and proposed functional differentiation of two repeated halves of the protein. *Crit. Rev. Biochem. Mol. Biol.* 28:235–257.

8. Verkman, A.S., A.N. van Hoek, T. Ma, A. Frigeri, W.R. Skach, A. Mitra, B.K. Tamarappoo, and J. Farinas. 1996. Water transport across mammalian cell membranes. *Am. J. Physiol.* 270:C12–C30.

9. Agre, P., G.M. Preston, B.L. Smith, J.S. Jung, S. Raina, C. Moon, W.B. Guggino, and S. Nielsen. 1993. Aquaporin CHIP: the archetypal molecular water channel. *Am. J. Physiol.* 265:F463–F476.

10. Matthay, M.A., H. Folkesson, and A.S. Verkman. 1996. Salt and water transport across alveolar and distal airway epithelia in the adult lung. *Am. J. Physiol.* In press.

11. Zhang, R., W. Skach, H. Hasegawa, A.N. van Hoek, and A.S. Verkman. 1993. Cloning, functional analysis and cell localization of a kidney proximal tubule water transporter homologous to CHIP28. *J. Cell Biol.* 120:359–369.

12. Nielsen, S., B.L. Smith, E.I. Christensen, and P. Agre. 1993. Distribution of the aquaporin CHIP in secretory and resorptive epithelia and capillary endothelia. *Proc. Natl. Acad. Sci. USA.* 90:7275–7279.

13. Hasegawa, H., R. Zhang, A. Dohrman, and A.S. Verkman. 1993. Tissue-specific expression of mRNA encoding the rat kidney water channel CHIP28k by *in situ* hybridization. *Am. J. Physiol.* 264:C237–C245.

14. Hasegawa, H., S.C. Lian, W.E. Finkbeiner, and A.S. Verkman. 1994. Extrarenal tissue distribution of CHIP28 water channels by *in situ* hybridization and antibody staining. *Am. J. Physiol.* 266:C893–C903.

15. Preston, G.M., B.L. Smith, M.L. Zeidel, J.J. Moulds, and P. Agre. 1994. Mutations in *aquaporin-1* in phenotypically normal humans without functional CHIP water channels. *Science (Wash. DC).* 265:1585–1587.

16. Fushimi, K., T. Uchida, Y. Hara, Y. Hirata, F. Marumo, and T. Sasaki. 1993. Cloning and expression of apical membrane water channel of rat kidney collecting tubule. *Nature (Lond.).* 361:549–552.

17. Ma, T., A. Frigeri, W. Skach, and A.S. Verkman. 1993. Cloning of a cDNA from rat kidney with homology to CHIP28 and WCH-CD water channels. *Biochem. Biophys. Res. Comm.* 197:654–659.

18. Hasegawa, H., T. Ma, W. Skach, M.A. Matthay, and A.S. Verkman. 1994. Molecular cloning of a mercurial-insensitive water channel expressed in selected water-transporting tissues. *J. Biol. Chem.* 269:5497–5500.

19. Yang, B., T. Ma, and A.S. Verkman. 1995. cDNA cloning, gene organization and chromosomal localization of a human mercurial-insensitive water channel: evidence for distinct transcriptional units. *J. Biol. Chem.* 270:22907–22913.

20. Frigeri, A., M. Gropper, C.W. Turck, and A.S. Verkman. 1995. Immunolocalization of the mercurial-insensitive water channel and glycerol intrinsic protein in epithelial cell plasma membranes. *Proc. Natl. Acad. Sci. USA.* 92: 4328–4331.

21. Frigeri, A., M. Gropper, F. Umenishi, M. Katsura, D. Brown, and A.S. Verkman. 1995. Localization of MIWC and GLIP water channel homologs in neuromuscular, epithelial and glandular tissues. *J. Cell Sci.* 108:2993–3002.

22. Ma, T., A. Frigeri, H. Hasegawa, and A.S. Verkman. 1994. Cloning of a water channel homolog expressed in brain meningeal cells and kidney collecting duct that functions as a stilbene-sensitive glycerol transporter. *J. Biol. Chem.* 269:21845–21849.

23. Ishibashi, K., S. Sasaki, K. Fushimi, S. Uchida, M. Kuwahara, H. Saito, T. Furukawa, K. Nakajima, Y. Yamaguchi, T. Gojobori, and F. Marumo. 1994. Molecular cloning and expression of a member of the aquaporin family with permeability to glycerol and urea in addition to water expressed at the basolateral membrane of kidney collecting duct cells. *Proc. Natl. Acad. Sci. USA.* 91: 6269–6273.

24. Echevarria, M., E.E. Windhager, S.S. Tate, and G. Frindt. 1994. Cloning and expression of AQP3, a water channel from the medullary collecting duct of rat kidney. *Proc. Natl. Acad. Sci. USA.* 91:10997–11001.

25. Raina, S., G.M. Preston, W.B. Guggino, and P. Agre. 1995. Molecular cloning and characterization of an aquaporin cDNA from salivary, lacrimal, and respiratory tissues. *J. Biol. Chem.* 270:1908–1912.

26. Kuwahara, M., C.A. Berry, and A.S. Verkman. 1988. Rapid development of vasopressin-induced hydroosmosis in kidney collecting tubules measured by a new fluorescence technique. *Biophys. J.* 54:595–602.

27. Kuwahara, M., L.B. Shi, F. Marumo, and A.S. Verkman. 1991. Transcellular water flow modulates water channel exocytosis and endocytosis in kidney collecting tubule. *J. Clin. Invest.* 88:423–429.

28. Kuwahara, M., and A.S. Verkman. 1988. Direct fluorescence measurement of diffusional water permeability in the vasopressin-sensitive kidney collecting tubule. *Biophys. J.* 54:587–593.

29. Finkelstein, A. 1987. Water Movement Through Lipid Bilayers, Pores, and Plasma Membranes: Theory and Reality. John Wiley & Sons, Inc. New York.

30. Verkman, A.S. 1993. Water channels. A volume *In* Molecular Biology Intelligence Series. R.G. Landes Company, Austin, Texas.

31. Zhang, R., and A.S. Verkman. 1991. Water and urea transport in *Xenopus* oocytes: expression of mRNA from toad urinary bladder. *Am. J. Physiol.* 260:C26–C34.

32. Shi, L.-B., K. Fushimi, and A.S. Verkman. 1991. Solvent drag measurement of transcellular and basolateral membrane NaCl reflection coefficient in mammalian proximal tubule. *J. Gen. Physiol.* 98:379–398.

33. Al-Bazzaz, F.J., C. Tarka, and M. Farah. 1991. Microperfusion of sheep bronchioles. *Am. J. Physiol.* 260:L594–L602.

34. Ballard, S.T., S.M. Schepens, J.C. Falcone, G.A. Meininger, and A.E. Taylor. 1992. Regional bioelectric properties of porcine airway epithelium. *J. Appl. Physiol.* 73:2021–2027.

35. Al-Bazzaz, F.J. 1994. Regulation of Na and Cl transport in sheep distal airways. *Am. J. Physiol.* 267:L193–L198.

36. Verkman, A.S. 1995. Optical methods to measure membrane transport processes. *J. Membr. Biol.* 148:99–110.

37. Macklem, P.T., D.F. Proctor, and J.C. Hogg. 1970. The stability of peripheral airways. *Respir. Physiol.* 8:191–196.

38. Yager, D., T. Cloutier, H. Feldman, J. Bastacky, J.M. Drazen, and R.D. Kamm. 1994. Airway surface liquid thickness as a function of lung volume in small airways of the guinea pig. *J. Appl. Physiol.* 77:2333–2340.

39. Matthay, M.A., and J.P. Wiener-Kronish. 1990. Intact epithelial barrier function is critical for the resolution of alveolar edema in humans. *Am. Rev. Respir. Dis.* 142:1250–1257.

40. Weibel, E.R. 1989. Lung morphometry and models in respiratory physiology. *In* Respiratory Physiology. H.K. Chang and M. Paiva, editors. Marcel Dekker Inc., New York. p. 1–56.

41. Baile, E.M., R.W. Dahlby, B.R. Wiggs, G.H. Parsons, and P.D. Pare. 1987. Effect of cold and warm dry air hyperventilation on canine airway blood flow. *J. Appl. Physiol.* 62:526–532.

42. Willumsen, N.J., C.W. Davis, and R.C. Boucher. 1994. Selective response of human airway epithelia to luminal but not serosal solution hypertonicity. Possible role for proximal airway epithelia as an osmolality transducer. *J. Clin. Invest.* 94:779–787.

43. Umenishi, F., A.S. Verkman and M. Gropper. 1996. Quantitative analysis of aquaporin mRNA expression in rat tissues. *DNA and Cell Biol.* In press.

44. Shi, L.-B., W.R. Skach, T. Ma, and A.S. Verkman. 1995. Distinct biogenesis mechanisms for water channels MIWC and CHIP28 at the endoplasmic reticulum. *Biochemistry.* 34:8250–8256.